



1 **Differences in instantaneous water use efficiency derived**
2 **from post-carboxylation fractionation respond to the**
3 **interaction of CO₂ concentrations and water stress in semi-**
4 **arid areas**

5 **Na Zhao¹, Ping Meng², Yabing He¹, Xinxiao Yu^{1*}**

6 ¹ College of soil and water conservation, Beijing Forestry University, Beijing 100083, P.R. China

7 ² Research Institute of Forestry, Chinese Academy of Forestry 100091, Beijing, P.R. China

8 **Abstract.** In the context of global warming attributable to the increasing levels of CO₂, severe
9 drought can be anticipated in areas with chronic water shortages (semi-arid areas), which
10 necessitates research on the interaction between elevated atmospheric concentrations of CO₂ and
11 drought on plant photosynthetic discrimination. As δ¹³C of water-soluble compounds in leaves was
12 depleted from extracellular CO₂ to primary assimilates, no explanation has been offered for ¹³C
13 fractionation before leaf-exported transportation of photosynthate. Either its variation according to
14 the CO₂ concentration and/or water stress gradients, or their interaction have not yet been identified.
15 Therefore, saplings of species typical to a semi-arid area of Northern China that have similar growth
16 status—*Platycladus orientalis* and *Quercus variabilis*—were selected and cultivated in growth
17 chambers with orthogonal treatments (four CO₂ concentrations [CO₂] × five soil volumetric water
18 contents (SWC)). The δ¹³C of water-soluble compounds extracted from leaves of potted saplings
19 was measured to determine the instantaneous water use efficiency (WUE_{cp}) after cultivation.
20 Instantaneous water use efficiency derived from gas exchange (WUE_{ge}) was integrated to estimate
21 differences in δ¹³C signal variation before leaf-exported translocation of primary assimilates. The
22 WUE_{ge} of the two saplings both decreased with increased soil moisture, and increased with elevated
23 [CO₂] at 35%–80% of Field Capacity (FC) by strengthening photosynthetic capacity and reducing
24 transpiration. Differences in instantaneous water use efficiency (iWUE) according to distinct
25 environmental changes differed between the species. The WUE_{ge} of *P. orientalis* was significantly
26 greater than that of *Q. variabilis*, while the opposite results were obtained in a comparison of the
27 WUE_{cp} of the two species. The differences between WUE_{ge} and WUE_{cp} were clearly species-
28 specific, as demonstrated in the interaction of [CO₂] and SWC. Rising [CO₂] coupled with
29 moistened soil generated increasing disparities between WUE_{ge} and WUE_{cp} in *P. orientalis* with an
30 amplitude of 0.0328‰–0.0472‰. Further, the differences between WUE_{ge} and WUE_{cp} of *Q.*
31 *variabilis* increased as CO₂ concentration increased and water stress alleviated (0.0384‰–
32 0.0466‰). The ¹³C fractionation in post-photosynthesis was linearly dependent on *g_s*, and was
33 attributed to environmental variation. Thus, cautious descriptions of the magnitude and
34 environmental dependence of apparent post-carboxylation fractionation are worth our attention in
35 photosynthetic fractionation.

36 **Key words:** Post-carboxylation fractionation; Carbon isotope fractionation; Elevated CO₂
37 concentration; Soil volumetric water content; Instantaneous water use efficiency



38 1 Introduction

39 Since the onset of the industrial revolution, the atmospheric CO₂ concentration has increased at
40 an annual rate of 0.4%, and is expected to increase further to 700 μmol·mol⁻¹, together with more
41 frequent periods of low water availability (IPCC, 2014). Increasing atmospheric CO₂ concentrations
42 that trigger an ongoing greenhouse effect will not only lead to fluctuations in global patterns of
43 precipitation, but also will amplify drought in arid regions, and lead to more frequent occurrences
44 of extreme drought events in humid regions (Lobell et al., 2014). Accompanying the increasing
45 concentration of CO₂, the mean δ¹³C of atmospheric CO₂ is depleted by 0.02‰–0.03‰ year⁻¹ (data
46 available from the CU-INSTAAR/NOAACMDL network for atmospheric CO₂;
47 <http://www.esrl.noaa.gov/gmd/>).

48 The carbon isotopic composition determined recently could respond more subtly to
49 environmental changes and their influences on diffusion via plant physiology and metabolic
50 processes (Gessler et al., 2014; Streit et al., 2013). While the depletion of δ¹³C_{CO₂} has been shown
51 in the atmosphere, variations in CO₂ concentration itself also might affect the δ¹³C of plant organs
52 that, in turn, respond physiologically to climatic change (Gessler et al., 2014). The carbon
53 discrimination (¹³Δ) of leaves could also provide timely feedback about the availability of soil
54 moisture and the atmospheric vapor pressure deficit (Cernusak et al., 2012). Discrimination against
55 ¹³C in leaves relies mainly on environmental factors that affect the ratio of intercellular to ambient
56 CO₂ concentration (*C_i/C_a*) and Rubisco activities (Farquhar et al., 1982). As changes in
57 environmental conditions affect photosynthetic discrimination, they are expected to be recorded
58 differentially in the δ¹³C of water-soluble organic matter (δ¹³C_{WSOM}) of the different plant organs.
59 Meanwhile, several processes during photosynthesis alter the δ¹³C of carbon transported within
60 plants considerably. Carbon-fractionation during photosynthetic CO₂ fixation has been described
61 and reviewed well elsewhere (Farquhar et al., 1982; Farquhar and Sharkey, 1982).

62 Post-photosynthetic fractionation is derived from equilibrium and kinetic isotopic effects, which
63 determines isotopic differences between metabolites and intramolecular reaction positions. Several
64 scholars have defined the carbon isotopic fractionations that occur between the leaf and wood
65 cambium as “post-photosynthetic” or “post-carboxylation” fractionation (Jäggi et al., 2002; Badeck
66 et al., 2005; Gessler et al., 2008). Post-carboxylation fractionation in plants includes the carbon
67 discriminations that follow carboxylation of ribulose-1, 5-bisphosphate, and internal diffusion
68 (RuBP, 27‰), as well as related transitory starch metabolism (Gessler et al., 2008; Gessler et al.,
69 2014), fractionation in leaves, fractionation-associated phloem transport, the remobilization or
70 storage of soluble carbohydrates, and starch metabolism fractionations in sink tissue (tree rings). In
71 sucrose synthesis, ¹³C-depletions of triose phosphates occur during exportation from the cytoplasm,
72 and during production of fructose-1, as does 6-bisphosphate by aldolase in transitory starch
73 synthesis (Rossmann et al., 1991; Gleixner and Schmidt, 1997). Synthesis of two sugars before
74 transportation to the twig is associated with the post-carboxylation fractionation generated in leaves.
75 It is also important to consider that the carbon cycling time within plants has an absolute influence
76 on the time integration of photosynthetic carbon discrimination. Several studies have indicated that
77 recently-assimilated carbohydrate that is imprinted with environmental signals is mixed with other
78 carbohydrate pools of different ages during transportation along the basipetal tree axis (Brandes et
79 al., 2006; Richardson et al., 2012). It is necessary to avoid confusion of carbon sources, and further,
80 to determine carbon fractionation within leaves following photosynthetic carboxylation. In addition,



81 whether these fractionations are related to environmental variation has not yet been investigated.

82 The simultaneous isotopic analysis of leaves is a recent refinement in isotope studies that allows
83 us to determine the temporal variation in isotopic fractionation (Rinne et al., 2016), and will help
84 decipher environmental conditions more reliably. Newly assimilated carbohydrates can be extracted,
85 and are defined as the water-soluble compounds (WSCs) in leaves (Brandes et al., 2006; Gessler et
86 al., 2009), which also can be associated with gas exchange properties on a daily basis (Kodama et
87 al., 2008). However, there is dispute whether the post-carboxylation fractionation process may alter
88 the stable signatures of leaf carbon and thence influence instantaneous water use efficiency (iWUE).
89 In addition, the way in which the iWUE derived from that isotope fractionation responds to different
90 environmental factors, such as elevated [CO₂] and/or soil water gradients, has not yet been observed.

91 Consequently, we investigated δ¹³C of the fast-turnover carbohydrate pool in leaves from saplings
92 of two trees typical in semi-arid areas of China—*Platycladus orientalis* and *Quercus variabilis*—
93 together with simultaneous gas exchange measurements in growth chambers (FH-230). Our goals
94 are to compare the differences in iWUE derived from ¹³C-fractionation of post-carboxylation
95 between *P. orientalis* and *Q. variabilis*, and to describe how these differences in iWUE respond to
96 the interactive effects of elevated [CO₂] and water stress.

97 2 Material and Methods

98 2.1 Study site and design

99 Saplings of *P. orientalis* and *Quercus variabilis* were selected as experimental material from the
100 Capital Circle forest ecosystem station, a part of the Chinese Forest Ecosystem Research Network
101 (CFERN, 40°03'45"N, 116°5'45"E) in Beijing, China. This region is populated by warm, temperate,
102 deciduous, broad-leaved trees and mixed tree communities dominated by *Quercus* spp. and
103 *Platycladus orientalis* (L.) Franco, respectively. Saplings have similar ground diameters, heights,
104 and growth statuses. The saplings were placed in pots 22 cm in diameter and 22 cm in height.
105 Undisturbed soil samples were collected from the field in the research region, and the sieved soil
106 (with all particles <10 mm removed) was placed in the pots. A single *P. orientalis* sapling was
107 transplanted into each pot. The soil bulk density in the pots was maintained at 1.337–1.447 g cm⁻³.
108 After one month of rejuvenation, the potted saplings were placed into chambers for cultivation.

109 The controlled experimental treatments were conducted in growth chambers (FH-230, Taiwan
110 Hipoint Corporation, Kaohsiung City, Taiwan). To imitate the meteorological factors of the growth
111 seasons in the research region, the daytime temperature in the chambers was set to 25 ± 0.5°C from
112 07:00 to 17:00, and the night-time temperature was 18 ± 0.5°C from 17:00 to 07:00. Relative
113 humidity was maintained at 60% and 80% during the day and night, respectively. The light system
114 was activated in the daytime and shut down at night. The average daytime light intensity was
115 maintained at 200–240 μmol m⁻² s⁻¹. CO₂ concentration was controlled by the central controlling
116 system of the chambers (FH-230). Two growth chambers (A and B) were used in our study.
117 Chamber A was switched in turn to maintain a CO₂ concentration of 400 ± 50 ppm (during June 2–
118 9, June 12–19, June 21–28, and July 2–9, 2015) and 500 ± 50 ppm (during July 11–18, July 22–29,
119 August 4–11, and August 15–22, 2015). The other was adjusted to maintain the CO₂ concentration
120 at 600 ± 50 ppm (during June 2–9, June 12–19, June 21–28, and July 2–9, 2015) and 800 ± 50 ppm
121 (during July 11–18, July 22–29, August 4–11, and August 15–22, 2015). The CO₂ concentration in
122 the chambers was set to maintain one target level (permitting a standard deviation of ± 50 ppm)



123 during cultivation. Thus, we employed a gradient of four CO₂ concentrations in our study (400 ± 50
124 ppm, 500 ± 50 ppm, 600 ± 50 ppm, and 800 ± 50 ppm). Detectors inside the chambers monitored
125 and maintained the CO₂ concentrations continuously at the constant setting.

126 We designed a device to water the potted plants automatically to avoid heterogeneity caused by
127 interruptions in the watering process (Fig. 1). It consisted of the water storage tank, holder,
128 controller, soil moisture sensors, and drip irrigation components. Prior to use, the water tank was
129 filled with water, and the soil moisture sensor was inserted to a uniform depth in the soil. After
130 connecting the controller to an AC power supply, specific soil water could be set. The soil
131 volumetric water content (SWC) of the pot soil was monitored by the soil moisture sensors. Through
132 the sensors, the chamber could determine whether to water or stop watering the plants. Two drip
133 irrigation devices were installed in both chambers, respectively. After measuring the average Field
134 Capacity (FC) of the pot soil (30.70%), five levels of SWC were maintained before the orthogonal
135 tests, as follows: 100% FC (or CK) (SWC approximately 27.63%–30.70%), 70%–80% of FC (SWC
136 approximately 21.49%–24.56%), 60%–70% of FC (SWC approximately 18.42%–21.49%), 50%–
137 60% of FC (SWC approximately 15.35%–18.42%), and 35%–45% of FC (SWC approximately
138 10.74%–13.81%). Each level of soil water was kept within the specific range thereafter by the
139 irrigation device.

140 After establishing the equilibrium circumstances of elevated CO₂ across the soil water gradients,
141 the saplings were ready for investigation. Each orthogonal treatment included three replicates, and
142 each replicate continued for 7 days. Pots were rearranged periodically to minimize non-uniform
143 illumination.

144 Orthogonal tests: elevated CO₂ concentration gradient presented as 400 ppm, 500 ppm, 600 ppm,
145 and 800 ppm, combined with a soil-water gradient 35%–45% of FC, 50%–60% of FC, 60%–70%
146 of FC, and 70%–80% of FC and 100% FC (CK).

147 2.2 Foliar gas exchange measurement

148 Fully expanded primary annual leaves of the saplings were measured with a portable infrared gas
149 photosynthesis system (LI-6400, Li-Cor, Lincoln, US) before and after the 7-day cultivation in the
150 chambers. The main photosynthetic parameters, such as net photosynthetic rate (P_n) and
151 transpiration rate (T_r), were measured. Based on the theories proposed by Von Caemmerer and
152 Farquhar (1981), stomatal conductance (g_s) and intercellular CO₂ concentration (C_i) were calculated
153 by the Li-Cor software. Each leaf was measured three times. Three leaves from each sapling were
154 chosen, and three saplings were measured within one orthogonal treatment. Instantaneous water use
155 efficiency via gas exchange (WUE_{ge}) was calculated as the ratio of P_n to E .

156 2.3 Plant material collection and sample preparation

157 After measuring gas exchange, recently-expanded, sun leaves were removed from the *P.*
158 *orientalis* and *Quercus variabilis* saplings cultivated in the orthogonal treatments, and frozen
159 immediately in liquid nitrogen. A protocol adapted from Gessler et al. (2004) was used to extract
160 the water-soluble compounds (WSCs). All samples were ground to fine powders using mortars and
161 liquid nitrogen. 50 mg of ground leaves and 100 mg PVPP (polyvinylpyrrolidone) were
162 weighed, mixed evenly, and incubated in 1ml double demineralized water for 60 min at 5°C in a
163 centrifuge tube. Then, the tubes were heated in 100°C water for 3 min. After they cooled to room
164 temperature, the supernatant was centrifuged at 12000 xg for 5 min and transferred into tin capsules



165 to be dried at 70°C. Folded capsules were then ready for $\delta^{13}\text{C}$ analysis of WSOM.

166 The samples of WSCs from leaves were combusted in an elemental analyzer (EuroEA,
 167 HEKATEch GmbH, Wegberg, Germany) and analyzed in the mass spectrometer (DELTA^{plus}XP,
 168 ThermoFinnigan). Carbon isotope signatures are expressed in δ -notation in parts per thousand,
 169 relative to the international Pee Dee Belemnite (PDB):

$$170 \quad \delta^{13}\text{C} = (R_{\text{sample}}/R_{\text{standard}}) \times 1000 \quad (1)$$

171 where $\delta^{13}\text{C}$ is the heavy isotope and R_{sample} and R_{standard} refer to the isotope ratio between
 172 the particular substance and the corresponding standard, respectively. The precision of the repeated
 173 measurements was 0.1 ‰.

174 2.4 Isotopic calculation

175 Based on the linear model developed by Farquhar and Sharkey (1982), the isotope discrimination
 176 factor, Δ , was calculated as:

$$177 \quad \Delta = (^{13}\text{C}_a - ^{13}\text{C}_p) / (1 + ^{13}\text{C}_p) \quad (2)$$

178 where $^{13}\text{C}_a$ is the isotope signature of ambient $[\text{CO}_2]$ in the chamber; $^{13}\text{C}_p$ is the $^{13}\text{C} : ^{12}\text{C}$ of
 179 the water-soluble compounds extracted from foliage. The $C_i : C_a$ is determined by:

$$180 \quad C_i : C_a = (\Delta - a) / (b - a) \quad (3)$$

181 where C_i is the intercellular CO_2 concentration, and C_a is the ambient CO_2 concentration in the
 182 chamber; a is the discrimination dependent on a fraction factor (4‰). b is the discrimination during
 183 CO_2 fixation by ribulose 1,5- bisphosphate carboxylase/oxygenase (Rubisco) and internal diffusion
 184 (27‰). Instantaneous water use efficiency (iWUE) is calculated as:

$$185 \quad \text{iWUE} = P_n : T_r = (C_a - C_i) / 1.6\Delta e \quad (4)$$

186 where P_n is the net carbon assimilation, T_r is the molar rate of transpiration, and 1.6 is the
 187 diffusion ratio of stomatal conductance to water vapor to CO_2 in the chamber. Δe is the difference
 188 in water vapor pressure between the intracellular in leaves and ambient air, which may be calculated
 189 as:

$$190 \quad \Delta e = e_{lf} - e_{atm} = 0.611 \times e^{17.502T/(240.97+T)} \times (1 - \text{RH}) \quad (5)$$

191 where e_{lf} and e_{atm} represent the extra- and intra- cellular water vapor pressure, respectively. T and
 192 RH is temperature and relative humidity on leaf surface.

$$193 \quad \text{WUE}_{\text{CP}} = \frac{P_n}{T_r} = (1 - \varphi) (C_a - C_i) / 1.6\Delta e = C_a (1 - \varphi) \left(1 - \frac{\delta^{13}\text{C}_a - \delta^{13}\text{C}_p - a}{(b - a)} \right) / 1.6\Delta e \quad (6)$$

194 φ is the ratio between carbohydrates consumed during respiration of the leaves and that of other
 195 organs at night (0.3).

196 3 Results

197 3.1 Foliar gas exchange measurements

198 *P. orientalis* and *Q. variabilis* saplings were exposed to the orthogonal treatments (under gradients
 199 of SWC and $[\text{CO}_2]$ of 400 ppm, 500 ppm, 600 ppm, and 800 ppm, labeled C₄₀₀, C₅₀₀, C₆₀₀, and C₈₀₀).
 200 When SWC increased, most P_n in *P. orientalis* peaked at 70%–80% of FC, while that of *Q. variabilis*
 201 reached higher values of 70%–80% of FC and FC. The uptake capacity of carbon was improved
 202 significantly with elevated $[\text{CO}_2]$ at any given soil moisture ($p < 0.05$) for *P. orientalis*. We observed



203 increased P_n of *Q. variabilis* after CO₂ gradient-fumigation, except under C₄₀₀. Further, greater
 204 magnitudes of increments in P_n of *P. orientalis* were found at 50%–70% of FC from C₄₀₀ to C₈₀₀,
 205 which was observed at 35%–45% of FC for *Q. variabilis*. Instantaneous carbon assimilation
 206 capacities of *Q. variabilis* among all treatments were stronger than were those of *P. orientalis* (Figs.
 207 2a and 2b, $p < 0.01$).

208 The g_s in *P. orientalis* coincided with P_n as soil moisture increased, and was highest at 70%–80%
 209 of FC in C₄₀₀, C₅₀₀, and C₈₀₀ (Fig. 2c), while it peaked at FC in C₆₀₀. When SWC increased from
 210 35%–45% to 50%–60% of FC, g_s in *Q. variabilis* moved up sharply and then increased gradually
 211 to its maximum in C₄₀₀, C₅₀₀, and C₈₀₀ as soil moisture increased. As the water stress was alleviated
 212 (at 70%–80% of FC and FC), the reduction of g_s in *P. orientalis* was more pronounced with elevated
 213 [CO₂] at a given SWC ($p < 0.01$). Nevertheless, g_s of *Q. variabilis* in C₄₀₀, C₅₀₀, and C₆₀₀ was
 214 significantly higher than that in C₈₀₀ at 50%–80% of FC ($p < 0.01$). g_s in *Q. variabilis* exceeded that
 215 in *P. orientalis* under the same treatments ($p < 0.01$, Figs. 2c and 2d).

216 The C_i in *P. orientalis* rose gradually as SWC increased, and peaked at FC at any given [CO₂].
 217 Under the same conditions of cultivation as *P. orientalis*, C_i of *Q. variabilis* reached their maximums
 218 at 60%–70% of FC, and declined thereafter with increased SWC. The variation in C_i of the two
 219 species was similar and decreased as [CO₂] elevated. C_i of *Q. variabilis* was significantly greater
 220 than was that of *P. orientalis* under the same treatment ($p < 0.01$, Figs. 2e and 2f).

221 The T_r of *P. orientalis* and *Q. variabilis* all exhibited single peaks that occurred at 70%–80% of
 222 FC in combination with the soil moisture gradient. The T_r of the two saplings in different [CO₂]
 223 were compared at each SWC (Figs. 2g and 2h). Except for 35%–60% of FC, the T_r of the two
 224 saplings in C₄₀₀ and C₅₀₀ was significantly higher than that in C₆₀₀ and C₈₀₀ ($p < 0.01$). With the same
 225 [CO₂] and the same SWC, the T_r of *Q. variabilis* was remarkably larger than was that of *P. orientalis*
 226 ($p < 0.01$).

227 3.2 $\delta^{13}\text{C}$ of water-soluble compounds in leaves

228 To observe the photosynthetic traits of the two saplings, the same leaf was frozen immediately
 229 and the water-soluble compounds (WSCs) were extracted for all orthogonal treatments. $\delta^{13}\text{C}_{\text{WSC}}$
 230 ($\delta^{13}\text{C}$ of water-soluble compounds from leaves) of *P. orientalis* and *Q. variabilis* saplings cultivated
 231 in the four CO₂ concentrations all increased as soil moisture improved (Figs. 3a and 3b, $p < 0.01$).
 232 The average (\pm SD) $\delta^{13}\text{C}_{\text{WSC}}$ values of *P. orientalis* and *Q. variabilis* ranged from $-27.44 \pm 0.155\%$
 233 to $-26.71 \pm 0.133\%$, and from $-27.96 \pm 0.129\%$ to $-26.49 \pm 0.236\%$, respectively. Further, we found
 234 that the average $\delta^{13}\text{C}_{\text{WSC}}$ of the two saplings reached their maximums at 70%–80% of FC in a given
 235 [CO₂]. Together with the gradual enrichment of [CO₂], trends of the average $\delta^{13}\text{C}_{\text{WSC}}$ values of the
 236 saplings declined when [CO₂] exceeded 600 ppm ($p < 0.01$). Except for C₄₀₀ at 50%–100% of FC,
 237 the $\delta^{13}\text{C}_{\text{WSC}}$ values of *P. orientalis* were significantly larger than were those of *Q. variabilis* for any
 238 other [CO₂] \times SWC treatments ($p < 0.01$).

239 3.3 Estimations of WUE_{ge} and WUE_{ep}

240 Instantaneous water use efficiency via gas exchange (WUE_{ge}) is calculated as P_n divided by T_r .
 241 Figure 4a shows that increased magnitudes of WUE_{ge} of *P. orientalis* under severe drought (i.e.,
 242 35%–45% of FC) were highest at any given [CO₂], ranging from 90.70% to 564.65%. As SWC
 243 increased, WUE_{ge} reduced along a gradient in C₄₀₀, C₅₀₀, C₆₀₀, and C₈₀₀, while they increased
 244 remarkably as [CO₂] increased. Compared to *P. orientalis*, the trends of WUE_{ge} in *Q. variabilis* were



245 promoted slightly at FC in C₆₀₀ or C₈₀₀ as soil water increased (Fig. 4b). The maximum of WUE_{ge}
246 in *P. orientalis* thus occurred at 35%–45% of FC in C₈₀₀ for all orthogonal treatments, and did so in
247 *Q. variabilis* as well. Further, elevated CO₂ concentrations enhanced the WUE_{ge} of *Q. variabilis*
248 clearly at any SWCs except that at 60%–80% of FC. Based on the comparison between the same
249 [CO₂] × SWC treatments, most saplings of *P. orientalis* had greater WUE_{ge} than did *Q. variabilis*
250 ($p < 0.05$).

251 The $\delta^{13}\text{C}$ values of water-soluble compounds from leaves of the two saplings were measured, and
252 the instantaneous water use efficiency could be determined from Eq. (6) for the $\delta^{13}\text{C}_{\text{WSC}}$ of leaves,
253 defined as WUE_{cp}. As illustrated in Fig. 5a, WUE_{cp} of *P. orientalis* in C₆₀₀ or C₈₀₀ climbed up as
254 water stress was reduced beyond 50%–60% of FC, while the water threshold was 60%–70% of FC
255 in C₄₀₀ or C₅₀₀. *Q. variabilis* exhibited no uniform trend of WUE_{cp} with soil wetting. Except for C₄₀₀,
256 WUE_{cp} of *Q. variabilis* decreased abruptly at 50%–60% of FC, and rose as soil moisture improved
257 in C₅₀₀, C₆₀₀, and C₈₀₀. Figure 5b shows the effects of elevated CO₂ on WUE_{cp} in *Q. variabilis*. In
258 contrast to the findings for WUE_{ge} in the two saplings, the WUE_{cp} of *Q. variabilis* was more
259 pronounced than was that of *P. orientalis* for all orthogonal treatments.

260 3.4 Post-carboxylation fractionation generated before photosynthate leaves the leaves

261 We evaluated the differences between instantaneous water use efficiency via leaf gas exchange
262 and $\delta^{13}\text{C}$ of water-soluble compounds (Table 1), which can retrace ¹³C fractionation before
263 carboxylation transport to the twig. When comparing WUE_{ge} and WUE_{cp}, the ¹³C-depletion of *P.*
264 *orientalis* ranged from 0.0328‰ to 0.0472‰, which was smaller than that of *Q. variabilis* (0.0384‰
265 to 0.0466‰). The fractionation effects of *P. orientalis* were magnified with increased soil moisture,
266 and particularly at 35%–80% of FC from C₄₀₀ to C₈₀₀, the magnitudes of the increments reached
267 21.30%–42.04%. Under C₄₀₀ and C₅₀₀ in *Q. variabilis*, the coefficients were amplified, as SWC
268 increased until 50%–60% of FC, then remained constant. With respect to C₆₀₀ and C₈₀₀, the
269 coefficients of *Q. variabilis* were amplified at 50%–80% of FC, and decreased at FC. The average
270 coefficients of *P. orientalis* increased gradually as [CO₂] rose, while those of *Q. variabilis* declined
271 sharply from C₆₀₀ to C₈₀₀. Coefficients of *P. orientalis* increased at a faster rate than did those of *Q.*
272 *variabilis* with increased soil moisture.

273 Stoma are the conduit between the plant and atmosphere. Post-carboxylation fractionation may
274 be correlated with the degree to which the stomata are open and the resistance they exert. Here, we
275 performed linear regressions between g_s and the ¹³C fractionation coefficient for *P. orientalis* and
276 *Q. variabilis* (Fig. 6). It was apparent that the ¹³C fractionation coefficient was linearly dependent
277 on the g_s ($p < 0.05$), which controls the exchange of CO₂ and H₂O, and responds to environmental
278 variation.

279 4 Discussion

280 4.1 Photosynthetic traits

281 The exchange of CO₂ and water vapor via stomata is modulated in part by the soil or leaf water
282 potential (Robredo et al., 2010). Saplings of *P. orientalis* reached their maximums of P_n and g_s at
283 70%–80% of FC under any [CO₂]. As SWC exceeded the water threshold, elevated CO₂ caused a
284 greater reduction in g_s , as has been reported for barley and wheat (Wall et al., 2011). Nonetheless,
285 maximal values of g_s in *Q. variabilis* in C₄₀₀, C₅₀₀, C₆₀₀, and C₈₀₀ were generated successively as
286 soil moisture increased, indicating that drought stimulated the stomata, which are more sensitive to



287 environmental changes. In addition, C_i of *Q. variabilis* peaked at 60%–70% of FC, following
288 declines as soil moisture increased (Wall et al., 2006; Wall et al., 2011). The g_s of *P. orientalis* and
289 *Q. variabilis* decreased with elevated $[\text{CO}_2]$, which was evidenced by FACE and non-FACE
290 experiments (Ainsworth and Rogers, 2007; Wall et al., 2011). This is interpreted as stomata having
291 the tendency to maintain a constant C_i or C_i/C_a when ambient $[\text{CO}_2]$ increases, which would
292 determine the CO_2 used directly in chloroplast (Yu et al., 2010). On the basis of theories proposed
293 by Farquhar and Sharkey (1982) and common experimental technologies (Xu, 1997), this could be
294 explained as a stomatal limitation. However, C_i of *P. orientalis* was observed to increase
295 considerably when SWC exceeded 70%–80% of FC in all CO_2 treatments (Mielke et al., 2000). One
296 factor that can account for this is that plants close their stomata to reduce intensive loss of water
297 during the synthesis of organic matter, simultaneously decreasing the availability of CO_2 and
298 generating respiration of organic matter (Robredo et al., 2007). Another explanation is that the
299 limited root volume in potted experiments may not be able to absorb sufficient water to support full
300 growth of shoots (Leakey et al., 2009; Wall et al., 2011). When SWC exceeds the threshold (70%–
301 80% of FC), further elevations in $[\text{CO}_2]$ may cause nonstomatal limitation, i.e., accumulation of
302 nonstructural carbohydrates in leaf tissue that induces mesophyll-based and/or biochemical-based
303 transient inhibition of photosynthetic capacity (Farquhar and Sharkey, 1982). Xu and Zhou (2011)
304 developed a five-level SWC gradient to examine the effect of water on the physiological and
305 ecological characteristics of perennial *Leymus chinensis*. They demonstrated that there was an
306 evident threshold in the gradient at which a plant could manage its structure and function to adjust
307 to environmental conditions. Miranda Apodaca et al. (2015) also concluded that, in suitable water
308 conditions, elevated CO_2 augmented CO_2 assimilation of herbaceous plants.

309 The P_n of the two saplings increased with increased $[\text{CO}_2]$ in our study, as was found previously
310 for C_3 in woody plants (Kgope et al., 2010). Further, increasing $[\text{CO}_2]$ appeared to alleviate soil
311 water stress at 35%–45% or 50%–60% of FC, which proves that photosynthetic inhibition produced
312 by water stress (or excess) may be moderated by increased $[\text{CO}_2]$ (Robredo et al., 2007; Robredo et
313 al., 2010). These results are consistent with a number of studies in which elevated CO_2 was expected
314 to ameliorate the adverse effects of drought stress by decreasing plant transpiration (Kirkham, 2016;
315 Kadam et al., 2014; Miranda Apodaca et al., 2015; Tausz Posch et al., 2013).

316 4.2 $\delta^{13}\text{C}$ of water-soluble compounds

317 Stable isotope ratios of plant tissues have been applied widely to evaluate the ecophysiological
318 processes that interact with environmental variation, especially those that control plant-atmosphere
319 exchanges of mass circulation and energy flow (McCarroll and Loader, 2004; Poussart et al., 2004;
320 Rinne et al., 2010). Based on the relationship between photosynthetic carbon isotope fractionation
321 ($\Delta^{13}\text{C}$ or Δ) and the ratio between internal leaf and ambient CO_2 concentration (C_i/C_a ; Eq. (2) and
322 Eq. (3), Farquhar et al. 1982), the $\delta^{13}\text{C}$ of plant tissue could characterize effects of environmental
323 interaction on internal reactions and processes of photosynthesis (Gessler et al., 2014). Further, the
324 leaf carbon isotope ratios are an excellent surrogate for direct measurement of iWUE (Eq. (4) shows
325 the determination of iWUE by $\delta^{13}\text{C}$), which was fractionated over CO_2 diffusion into leaf via
326 stomata and carboxylation in chloroplast. The $\delta^{13}\text{C}$ of water-soluble compounds ($\delta^{13}\text{C}_{\text{WSC}}$) extracted
327 from saplings' leaves has been measured to examine the physiological and metabolic responses to
328 current environmental variation (Streit et al., 2013). The authors found that the average $\delta^{13}\text{C}_{\text{WSC}}$ of
329 *P. orientalis* and *Q. variabilis* were correlated positively with the increment of soil moisture during



330 35%–80% of FC, which was demonstrated by Adiredjo et al. (2014) as well. Thus, $\delta^{13}\text{C}_{\text{WSC}}$ may
331 respond according to the availability of soil moisture, which was reviewed by Cernusak et al. (2012).
332 Once it exceeds 70%–80% of FC, the average $\delta^{13}\text{C}_{\text{WSC}}$ values of the two saplings with soil
333 moistening were consistent with the trends of g_s . Elevated CO_2 concentrations affected
334 physiological performance profoundly (Gimeno et al., 2015), especially by increasing the CO_2
335 supply to the chloroplasts and reducing stomatal conductance, which would have influenced
336 $\delta^{13}\text{C}_{\text{WSC}}$ indirectly in this study.

337 4.3 Differences between WUE_{ge} and WUE_{cp}

338 The increments of WUE_{ge} in *P. orientalis* and *Q. variabilis* that resulted from the combination of
339 an increase in P_n and decrease in g_s , followed by the reduction of T_r (Figs. 1a, 1g, 1b and 1h), also
340 were demonstrated by Ainsworth and McGrath (2010). Combining the P_n and T_r of *P. orientalis* and
341 *Q. variabilis* in the same treatment, the lower WUE_{ge} in *Q. variabilis* is achieved generally by the
342 plant's physiological and morphological traits, such as larger leaf area, rapid growth, and higher
343 stomatal conductance than that of *P. orientalis* (Adiredjo et al., 2014). Medlyn et al. (2001) reported
344 that the stomatal conductance of broadleaved species is more sensitive to elevated CO_2
345 concentrations than is that of conifers. Moreover, with respect to the patterns of iWUE , there has
346 been no consensus on soil water states at the leaf level, although some have discussed this topic
347 (Yang et al., 2010). As SWC decreased, the WUE_{ge} of *P. orientalis* and *Q. variabilis* was enhanced,
348 as presented by Parker and Pallardy (1991), DeLucia and Heckathorn (1989), and Reich et al. (1989).
349 Leakey (2009) also concluded that the WUE of stressed plants could be increased substantially,
350 which was shown more clearly with elevated $[\text{CO}_2]$ in this study.

351 Böggelein et al. (2012) confirmed that WUE_{cp} was more consistent with daily mean WUE_{ge} than
352 was $\text{WUE}_{\text{phloem}}$. The WUE_{cp} of *P. orientalis* and *Q. variabilis* demonstrated similar variations to
353 those of $\delta^{13}\text{C}_{\text{WSC}}$, and water stress was alleviated when combined with elevated $[\text{CO}_2]$, which
354 differentiated the trends in WUE_{ge} . The assumption has been made that $\delta^{13}\text{C}_{\text{WSC}}$ is coupled tightly
355 with dynamics in the environment several days before the water-soluble compounds is extracted.
356 As observed, the WUE_{cp} of *P. orientalis* and *Q. variabilis* responded synthetically with increasing
357 SWC across different $[\text{CO}_2]$ gradients over the course of several days. Consequently, WUE_{cp} and
358 WUE_{ge} have different variable curves according to treatments. In addition, there were characteristic
359 species-specific responses of $\delta^{13}\text{C}_{\text{WSC}}$ under the same environmental conditions.

360 4.4 Post-carboxylation fractionation generated before photosynthate leaving leaves

361 Photosynthesis, a biochemical and physiological process (Badeck et al., 2005), is characterized
362 by discrimination against ^{13}C , which leaves an isotopic signature in the photosynthetic apparatus.
363 There is already a classic review of the carbon-fractionation in leaves (Farquhar et al., 1989) that
364 covers the significant aspects of photosynthetic carbon isotope discrimination. The transportation
365 route of photosynthate production, from leaf to wood formation, consists of post-assimilation
366 fractionations/processes, referred to as “post-photosynthetic” or “post-carboxylation” fractionation
367 (Jäggi et al., 2002; Gessler et al., 2008). The post-photosynthetic fractionation associated with the
368 metabolic pathways of non-structural carbohydrates (NSC; defined here as soluble sugars + starch)
369 within leaves, and fractionation during translocation, storage, and remobilization prior to tree ring
370 formation remain unclear (Epron et al., 2012; Gessler et al., 2014; Rinne et al., 2016). The synthetic
371 processes of sucrose and starch before transportation to the twig are within the domain of post-



372 carboxylation fractionation generated in leaves. Hence, we hypothesized that ^{13}C fractionation
373 might exist. The WUE_{ge} of the plant responds to instantaneous carbon assimilation and transpiration.
374 When we finished the leaf gas exchange measurements, the leaf samples were collected immediately
375 to determine the $\delta^{13}\text{C}$ of water-soluble compounds (WUE_{cp}). Presumably, the ^{13}C fractionation
376 generated in the synthetic processes of sucrose and starch was approximately equal to the $\delta^{13}\text{C}$
377 difference between WUE_{ge} and WUE_{cp} . When comparing WUE_{ge} and WUE_{cp} , the ^{13}C -depletion of
378 *P. orientalis* ranged from 0.0328‰ to 0.0472‰, less than that of *Q. variabilis* (from 0.0384‰ to
379 0.0466‰). Recently, Gessler et al. (2004) reviewed the environmental drivers of variation in
380 photosynthetic carbon isotope discrimination in terrestrial plants. The ^{13}C fractionation effects of *P.*
381 *orientalis* were enhanced by soil moistening, consistent with that of *Q. variabilis*, except at FC. The
382 ^{13}C isotope signature of *P. orientalis* was dampened by elevated $[\text{CO}_2]$. Yet, ^{13}C -depletion was
383 weakened in *Q. variabilis* in C_{600} and C_{800} . Linear regression between g_s and the ^{13}C fractionation
384 coefficient indicated that the post-carboxylation fractionation in leaves depended on the variation
385 of g_s and stomata aperture correlated with environmental change.

386 5 Conclusions

387 Through orthogonal treatments of four $[\text{CO}_2]$ \times five SWC, WUE_{cp} calculated by $\delta^{13}\text{C}$ of water-
388 soluble compound and WUE_{ge} derived from simultaneous leaf gas exchange for leaves were
389 estimated to differentiate the $\delta^{13}\text{C}$ signal variation before leaf-exported translocation of primary
390 assimilates. In response to the interactive effects of $[\text{CO}_2]$ and SWC, WUE_{ge} of the two species of
391 saplings both decreased with soil moistening, and increased with elevated $[\text{CO}_2]$ at 35%–80% of
392 FC. We concluded that relative soil drying, coupled with elevated $[\text{CO}_2]$, could improve WUE_{ge} by
393 strengthening photosynthetic capacity and reducing transpiration. WUE_{ge} of *P. orientalis* was
394 significantly greater than was that of *Q. variabilis*, while the opposite was the case for WUE_{cp}
395 in the two species. Rising $[\text{CO}_2]$ and/or soil moistening generated increasing disparities between
396 WUE_{ge} and WUE_{cp} in *P. orientalis*; nevertheless, the differences between WUE_{ge} and WUE_{cp} in *Q.*
397 *variabilis* increased as $[\text{CO}_2]$ increased and/or water stress was alleviated. The ^{13}C fractionation also
398 was linearly dependent on g_s . With respect to post-photosynthesis fractionation in post-
399 carboxylation and transportation processes, we cannot neglect the fact that the instantaneous water
400 use efficiency derived from the synthesis of sucrose and starch were influenced inevitably by
401 environmental changes. Thus, cautious descriptions of the magnitude and environmental
402 dependence of apparent post-carboxylation fractionation are worth our attention in photosynthetic
403 fractionation.

404 References

- 405 Adiredjo, A. L., Navaud, O., Lamaze, T., and Grieu, P.: Leaf carbon isotope discrimination as an accurate
406 indicator of water use efficiency in sunflower genotypes subjected to five stable soil water contents,
407 J Agron. Crop Sci., 200, 416–424, 2014.
- 408 Ainsworth, E. A. and McGrath, J. M.: Direct effects of rising atmospheric carbon dioxide and ozone on
409 crop yields, Climate Change and Food Security, Springer, 109–130, 2010.
- 410 Ainsworth, E. A. and Rogers, A.: The response of photosynthesis and stomatal conductance to rising
411 $[\text{CO}_2]$: mechanisms and environmental interactions, Plant Cell Environ., 30, 258–270, 2007.
- 412 Badeck, F. W., Tcherkez, G., Eacute, N. S. S., Piel, C. E. M., and Ghashghaie, J.: Post-photosynthetic
413 fractionation of stable carbon isotopes between plant organ – a widespread phenomenon, Rapid



- 414 Commun. Mass S., 19, 1381–1391, 2005.
- 415 Bögelein, R., Hassdenteufel, M., Thomas, F. M., and Werner, W.: Comparison of leaf gas exchange and
 416 stable isotope signature of water-soluble compounds along canopy gradients of co-occurring
 417 Douglas-fir and European beech, *Plant Cell Environ.*, 35, 1245–1257, 2012.
- 418 Brandes, E., Kodama, N., Whittaker, K., Weston, C., Rennenberg, H., Keitel, C., Adams, M. A., and
 419 Gessler, A.: Short-term variation in the isotopic composition of organic matter allocated from the
 420 leaves to the stem of *Pinus sylvestris*: effects of photosynthetic and postphotosynthetic carbon
 421 isotope fractionation, *Global Change Biol.*, 12, 1922–1939, 2006.
- 422 Cernusak, L. A., Ubierna, N., Winter, K., Holtum, J. A. M., Marshall, J. D., and Farquhar, G. D.:
 423 Environmental and physiological determinants of carbon isotope discrimination in terrestrial plants,
 424 *Indian Journal of Science & Technology*, 94, 49–53, 2012.
- 425 DeLucia, E. H. and Heckathorn, S. A.: The effect of soil drought on water-use efficiency in a contrasting
 426 Great Basin desert and Sierran montane species, *Plant Cell Environ.*, 12, 935–940, 1989.
- 427 Epron, D., Nouvellon, Y., and Ryan, M. G.: Introduction to the invited issue on carbon allocation of trees
 428 and forests, *Tree physiol.*, 32, 639–643, 2012.
- 429 Farquhar, G. D., And, J. R. E., and Hubick, K. T.: Carbon isotope discrimination and photosynthesis,
 430 *Ann. Rev. Plant Physiol. Mol. Biol.*, 40, 503–537, 1989.
- 431 Farquhar, G. D., O'Leary, M. H., and Berry, J. A.: On the relationship between carbon isotope
 432 discrimination and the intercellular carbon dioxide concentration in leaves, *Funct. Plant Biol.*, 9,
 433 121–137, 1982.
- 434 Farquhar, G. D. and Sharkey, T. D.: Stomatal conductance and photosynthesis, *Ann. Rev. Plant Physiol.*,
 435 33, 317–345, 1982.
- 436 Gessler, A., Brandes, E., Buchmann, N., Helle, G., Rennenberg, H., and Barnard, R. L.: Tracing carbon
 437 and oxygen isotope signals from newly assimilated sugars in the leaves to the tree-ring archive,
 438 *Plant Cell Environ.*, 32, 780–795, 2009.
- 439 Gessler, A., Ferrio, J. P., Hommel, R., Treydte, K., Werner, R. A., and Monson, R. K.: Stable isotopes
 440 in tree rings: towards a mechanistic understanding of isotope fractionation and mixing processes
 441 from the leaves to the wood, *Tree Physiol.*, 34, 796–818, 2014.
- 442 Gessler, A., Rennenberg, H., and Keitel, C.: Stable isotope composition of organic compounds
 443 transported in the phloem of European beech-evaluation of different methods of phloem sap
 444 collection and assessment of gradients in carbon isotope composition during leaf-to-stem transport,
 445 *Plant Biology*, 6, 721–729, 2004.
- 446 Gessler, A., Tcherkez, G., Peuke, A. D., Ghashghaie, J., and Farquhar, G. D.: Experimental evidence for
 447 diel variations of the carbon isotope composition in leaf, stem and phloem sap organic matter in
 448 *Ricinus communis*, *Plant Cell Environ.*, 31, 941–953, 2008.
- 449 Gimeno, T. E., Crous, K. Y., Cooke, J., O'Grady, A. P., Ósváldsson, A., Medlyn, B. E., and Ellsworth,
 450 D. S.: Conserved stomatal behavior under elevated CO₂ and varying water availability in a mature
 451 woodland, *Funct. Ecol.*, 30, 700–709, 2015.
- 452 Gleixner, G. and Schmidt, H.: Carbon isotope effects on the fructose-1, 6-bisphosphate aldolase reaction,
 453 origin for non-statistical ¹³C distributions in carbohydrates, *J. Biol. Chem.*, 272, 5382–5387, 1997.
- 454 IPCC: Summary for policymakers, in: *Climate Change 2014, Mitigation of Climate Change*, contribution
 455 of Working Group III to the Fifth Assessment Report of the Intergovernmental Panel on Climate
 456 Change, edited by: Edenhofer, O., Pichs-Madruga, R., Sokona, Y., Farahani, E., Kadner, S., Seyboth,
 457 K., Adler, A., Baum, I., Brunner, S., Eickemeier, P., Kriemann, B., Savolainen, J., Schlömer, S.,



- 458 von Stechow, C., Zwickel, T., and Minx, J. C., Cambridge University Press, Cambridge, UK and
 459 New York, NY, USA, 1–30, 2014.
- 460 Jäggi, M., Saurer, M., Fuhrer, J., and Siegwolf, R.: The relationship between the stable carbon isotope
 461 composition of needle bulk material, starch, and tree rings in *Picea abies*, *Oecologia*, 131, 325–332,
 462 2002.
- 463 Kadam, N. N., Xiao, G., Melgar, R. J., Bahuguna, R. N., Quinones, C., Tamilselvan, A., Prasad, P. V.
 464 V., and Jagadish, K. S. V.: Chapter three-agronomic and physiological responses to high
 465 temperature, drought, and elevated CO₂ interactions in cereals, *Adv. Agron.*, 127, 111–156, 2014.
- 466 Kgope, B. S., Bond, W. J., and Midgley, G. F.: Growth responses of African savanna trees implicate
 467 atmospheric [CO₂] as a driver of past and current changes in savanna tree cover, *Austral Ecol.*, 35,
 468 451–463, 2010.
- 469 Kirkham, M. B.: *Elevated carbon dioxide: impacts on soil and plant water relations*, CRC Press, London,
 470 New York, 2016.
- 471 Kodama, N., Barnard, R. L., Salmon, Y., Weston, C., Ferrio, J. P., Holst, J., Werner, R. A., Saurer, M.,
 472 Rennenberg, H., and Buchmann, N.: Temporal dynamics of the carbon isotope composition in a
 473 *Pinus sylvestris* stand: from newly assimilated organic carbon to respired carbon dioxide, *Oecologia*,
 474 156, 737–750, 2008.
- 475 Leakey, A. D.: Rising atmospheric carbon dioxide concentration and the future of C4 crops for food and
 476 fuel, *Proceedings of the Royal Society of London B: Biological Sciences*, 276, 1517–2008, 2009.
- 477 Leakey, A. D., Ainsworth, E. A., Bernacchi, C. J., Rogers, A., Long, S. P., and Ort, D. R.: Elevated CO₂
 478 effects on plant carbon, nitrogen, and water relations: six important lessons from FACE, *J. Exp.*
 479 *Bot.*, 60, 2859–2876, 2009.
- 480 Lobell, D. B., Roberts, M. J., Schlenker, W., Braun, N., Little, B. B., Rejesus, R. M., and Hammer, G.
 481 L.: Greater sensitivity to drought accompanies maize yield increase in the US Midwest, *Science*,
 482 344, 516–519, 2014.
- 483 McCarroll, D. and Loader, N. J.: Stable isotopes in tree rings, *Quaternary Sci. Rev.*, 23, 771–801, 2004.
- 484 Medlyn, B. E., Barton, C. V. M., Broadmeadow, M. S. J., Ceulemans, R., Angelis, P. D., Forstreuter, M.,
 485 Freeman, M., Jackson, S. B., Kellomäki, S., and Laitat, E.: Stomatal conductance of forest species
 486 after long-term exposure to elevated CO₂ concentration: a synthesis, *New Phytol.*, 149, 247–264,
 487 2001.
- 488 Mielke, M. S., Oliva, M. A., de Barros, N. F., Penchel, R. M., Martinez, C. A., Da Fonseca, S., and de
 489 Almeida, A. C.: Leaf gas exchange in a clonal eucalypt plantation as related to soil moisture, leaf
 490 water potential and microclimate variables, *Trees*, 14, 263–270, 2000.
- 491 Miranda Apodaca, J., Pérez López, U., Lacuesta, M., Mena Petite, A., and Muñoz Rueda, A.: The type
 492 of competition modulates the ecophysiological response of grassland species to elevated CO₂ and
 493 drought, *Plant Biol.*, 17, 298–310, 2015.
- 494 Parker, W. C. and Pallardy, S. G.: Gas exchange during a soil drying cycle in seedlings of four black
 495 walnut (*Juglans nigra* L.) Families, *Tree physiol.*, 9, 339–348, 1991.
- 496 Poussart, P. F., Evans, M. N., and Schrag, D. P.: Resolving seasonality in tropical trees: multi-decade,
 497 high-resolution oxygen and carbon isotope records from Indonesia and Thailand, *Earth Planet. Sc.*
 498 *Lett.*, 218, 301–316, 2004.
- 499 Reich, P. B., Walters, M. B., and Tabone, T. J.: Response of *Ulmus americana* seedlings to varying
 500 nitrogen and water status. 2 Water and nitrogen use efficiency in photosynthesis, *Tree Physiol.*, 5,
 501 173–184, 1989.



- 502 Richardson, A. D., Carbone, M. S., Keenan, T. F., Czimczik, C. I., Hollinger, D. Y., Murakami, P.,
 503 Schaberg, P. G., and Xu, X.: Seasonal dynamics and age of stemwood nonstructural carbohydrates
 504 in temperate forest trees, *New Phytol.*, 197, 850–861, 2012.
- 505 Rinne, K. T., Loader, N. J., Switsur, V. R., Treydte, K. S., and Waterhouse, J. S.: Investigating the
 506 influence of sulphur dioxide (SO₂) on the stable isotope ratios (δ¹³C and δ¹⁸O) of tree rings, *Geochim.*
 507 *Cosmochim.*, 74, 2327–2339, 2010.
- 508 Rinne, K. T., Saurer, M., Kirilyanov, A. V., Bryukhanova, M. V., Prokushkin, A. S., Churakova Sidorova,
 509 O. V., and Siegwolf, R. T.: Examining the response of larch needle carbohydrates to climate using
 510 compound-specific δ¹³C and concentration analyses, EGU General Assembly Conference,
 511 1814949R, 2016.
- 512 Robredo, A., Pérez-López, U., de la Maza, H. S., González-Moro, B., Lacuesta, M., Mena-Petite A., and
 513 Muñoz-Rueda, A.: Elevated CO₂ alleviates the impact of drought on barley improving water status
 514 by lowering stomatal conductance and delaying its effects on photosynthesis, *Environ. Exp. Bot.*,
 515 59, 252–263, 2007.
- 516 Robredo, A., Pérez-López, U., Lacuesta, M., Mena-Petite, A., and Muñoz-Rueda, A.: Influence of water
 517 stress on photosynthetic characteristics in barley plants under ambient and elevated CO₂
 518 concentrations, *Biologia. Plantarum*, 54, 285–292, 2010.
- 519 Rossmann, A., Butzenlechner, M., and Schmidt, H.: Evidence for a nonstatistical carbon isotope
 520 distribution in natural glucose, *Plant Physiol.*, 96, 609–614, 1991.
- 521 Streit, K., Rinne, K. T., Hagedorn, F., Dawes, M. A., Saurer, M., Hoch, G., Werner, R. A., Buchmann,
 522 N., and Siegwolf, R. T. W.: Tracing fresh assimilates through *Larix decidua* exposed to elevated
 523 CO₂ and soil warming at the alpine treeline using compound-specific stable isotope analysis, *New*
 524 *Phytol.*, 197, 838–849, 2013.
- 525 Tausz Posch, S., Norton, R. M., Seneweera, S., Fitzgerald, G. J., and Tausz, M.: Will intra-specific
 526 differences in transpiration efficiency in wheat be maintained in a high CO₂ world? A FACE study,
 527 *Physiol. Plantarum*, 148, 232–245, 2013.
- 528 Von Caemmerer, S. V. and Farquhar, G. D.: Some relationships between the biochemistry of
 529 photosynthesis and the gas exchange of leaves, *Planta*, 153, 376–387, 1981.
- 530 Wall, G. W., Garcia, R. L., Kimball, B. A., Hunsaker, D. J., Pinter, P. J., Long, S. P., Osborne, C. P.,
 531 Hendrix, D. L., Wechsung, F., and Wechsung, G.: Interactive effects of elevated carbon dioxide and
 532 drought on wheat, *Agron. J.*, 98, 354–381, 2006.
- 533 Wall, G. W., Garcia, R. L., Wechsung, F., and Kimball, B. A.: Elevated atmospheric CO₂ and drought
 534 effects on leaf gas exchange properties of barley, *Agr. Ecosyst. Environ.*, 144, 390–404, 2011.
- 535 Xu, D. Q.: Some problems in stomatal limitation analysis of photosynthesis, *Plant Physiol. J.*, 33, 241–
 536 244, 1997.
- 537 Xu, Z. and Zhou, G.: Responses of photosynthetic capacity to soil moisture gradient in perennial rhizome
 538 grass and perennial bunchgrass, *BMC Plant Boil.*, 11, 21, 2011.
- 539 Yang, B., Pallardy, S. G., Meyers, T. P., GU, L. H., Hanson, P. J., Wullschleger, S. D., Heuer, M.,
 540 Hosman, K. P., Riggs, J. S., and Sluss D. W.: Environmental controls on water use efficiency during
 541 severe drought in an Ozark Forest in Missouri, USA, *Global Change Biol.*, 16, 2252–2271, 2010.
- 542 Yu, G., Wang, Q., and Mi, N.: *Ecophysiology of plant photosynthesis, transpiration, and water use*,
 543 Science Press, Beijing, China, 2010.
- 544
- 545



546

547 **Author contribution**

548 Na Zhao and Yabing He collected field samples, and performed the experiment. Na Zhao engaged
549 in data analysis and writing this paper. Ping Meng proposed the suggestions on the theory and
550 practice of experiment. Xinxiao Yu revised the paper and contributed to edit the manuscript.

551

552 *Acknowledgements.* We would like to thank Beibei Zhou and Yuanhai Lou for kind support in the
553 collection of materials and management of saplings. We are grateful to anonymous reviewers for
554 constructive suggestions of this manuscript. Due to the limitation of space allowed, we cited a part
555 of literatures involving this study area and apologized for authors whose work has not been cited.
556 All authors acknowledges support of National Natural Science Foundation of China (grant No.
557 41430747).

558

559

560

561

562

563

564

565

566

567

568

569

570

571

572

573

574

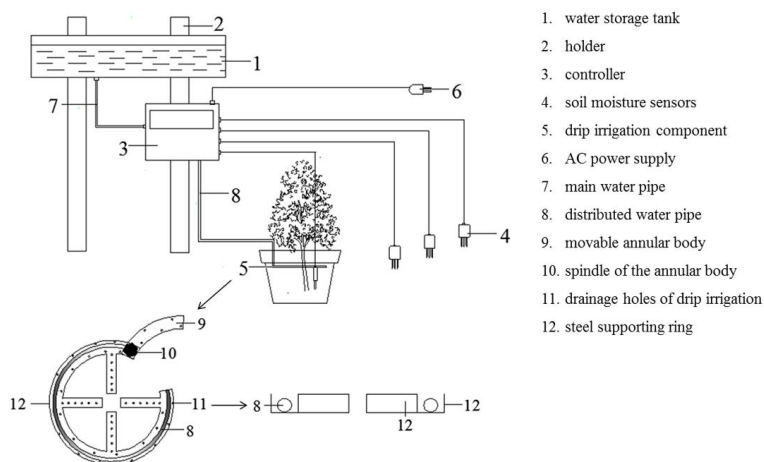
575

576

577

578

579



580

581 **Figure 1.** Structural diagram of the device for automatic drip irrigation

582 Arabic numerals indicate the individual parts of the automatic drip irrigation device (No. 1–7). The
583 lower-left corner of this figure presents the detailed schematic for the drip irrigation components (No. 8–
584 12). The lower-right corner of this figure shows the schematic for the drip irrigation component in profile.

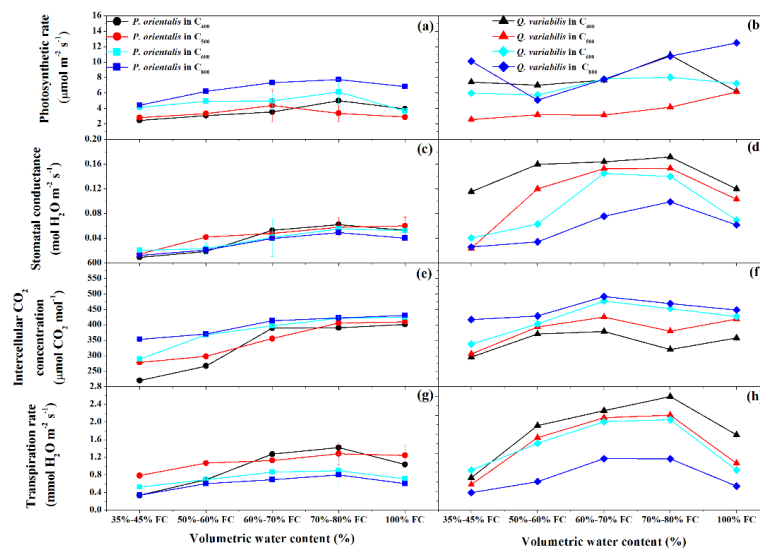
585

586

587

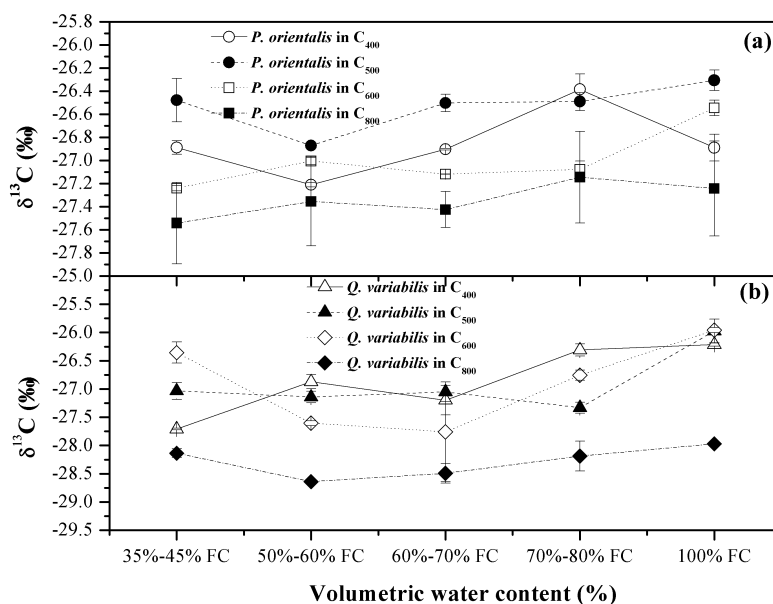
588

589



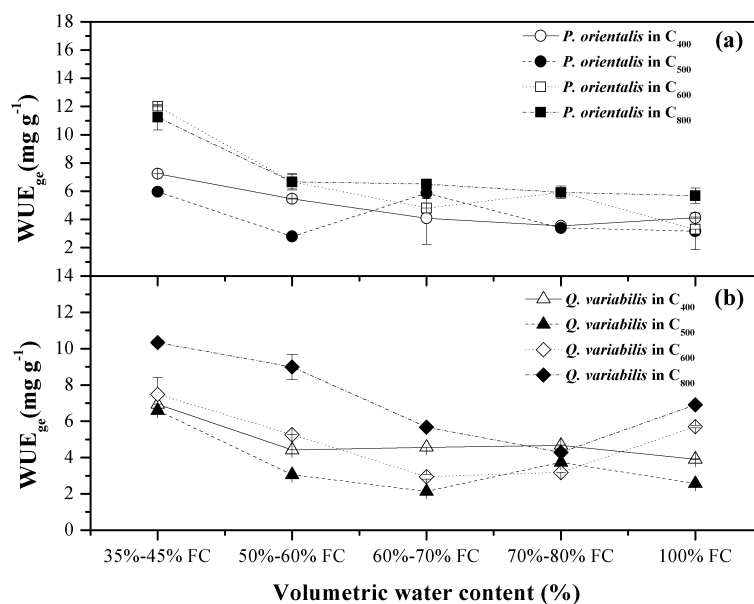
590

591 **Figure 2.** Photosynthetic parameters of *P. orientalis* and *Q. variabilis* saplings in CO₂
 592 concentrations of 400 ppm, 500 ppm, 600 ppm and 800 ppm across five soil volumetric water
 593 contents. The net photosynthetic rates (P_n , $\mu\text{mol m}^{-2} \text{s}^{-1}$), stomatal conductance (g_s , $\text{mol H}_2\text{O m}^{-2} \text{s}^{-1}$),
 594 intercellular CO₂ concentration (C_i , $\mu\text{mol CO}_2 \text{ mol}^{-1}$), and transpiration rates (T_r , $\text{mmol H}_2\text{O m}^{-2} \text{s}^{-1}$)
 595 are shown in Figs. 2a and 2b, 2c and 2d, 2e and 2g, and 2g and 2h, respectively. Means \pm
 596 SDs, $n = 32$.

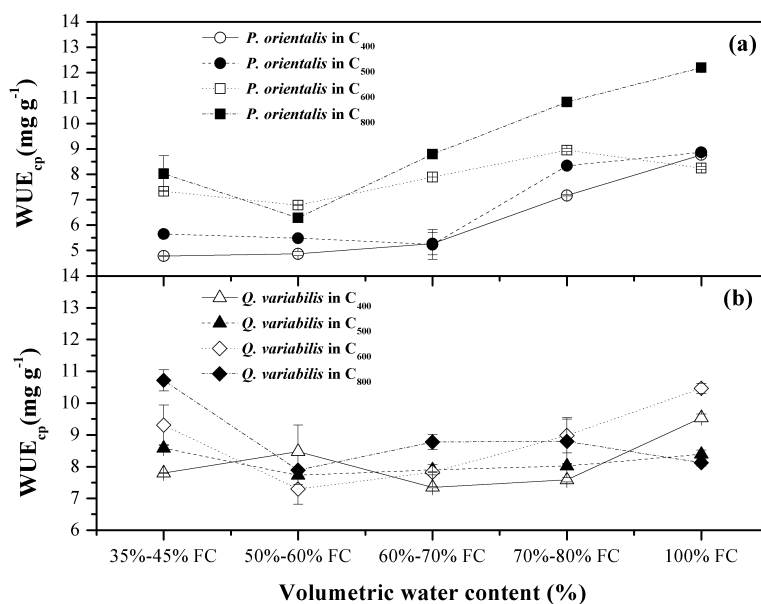


597

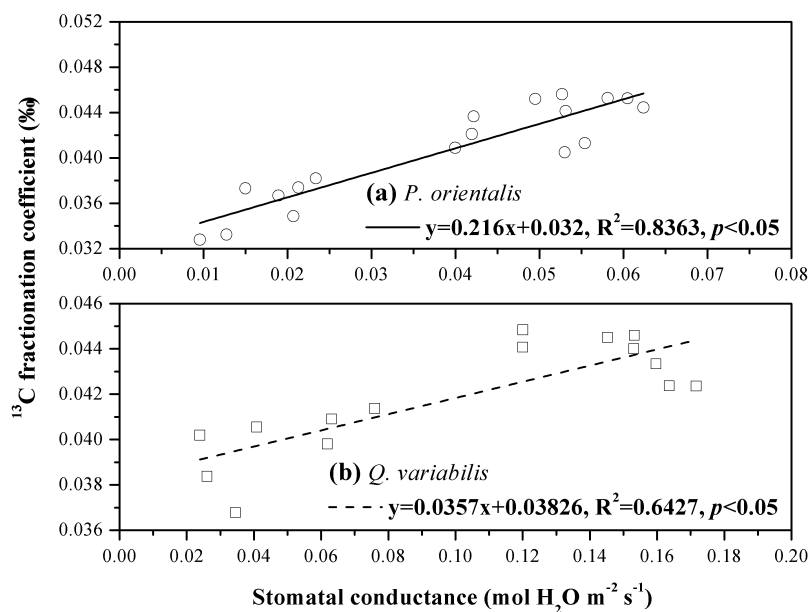
598 **Figure 3.** δ¹³C of water-soluble compounds extracted from leaves of *P. orientalis* and *Q. variabilis*
 599 cultivated in CO₂ concentrations of 400 ppm, 500 ppm, 600 ppm and 800 ppm across five soil
 600 volumetric water contents are shown in Figs. 3a and 3b. Means ±SDs, n = 32.



601
602 **Figure 4.** Instantaneous water use efficiency through gas exchange (WUE_{ge}) in leaves of *P.*
603 *orientalis* and *Q. variabilis* cultivated in CO₂ concentrations of 400 ppm, 500 ppm, 600 ppm and
604 800 ppm across five soil volumetric water contents are shown in Figs. 4a and 4b. Means ± SDs, n =
605 32.



606
607 **Figure 5.** Instantaneous water use efficiency through $\delta^{13}\text{C}$ of water-soluble compounds (WUE_{cp}) in
608 leaves of *P. orientalis* and *Q. variabilis* cultivated in CO_2 concentrations of 400 ppm, 500 ppm, 600
609 ppm, and 800 ppm across five soil volumetric water contents are shown in Figs. 5a and 5b. Means
610 \pm SDs, $n = 32$.



611

612 **Figure 6.** Regression between stomatal conductance and ^{13}C fractionation coefficient of *P. orientalis*
 613 and *Q. variabilis* under four CO_2 concentrations \times five soil volumetric water contents are
 614 established in Figs. 6a and 6b. $p = 0.05$, $n = 32$.

615

616

617

618

619

620

621

622

623

624

625

626

627

628

629

630

631

632

633

634



635 **Table 1.** ^{13}C fractionation coefficients of *P. orientalis* and *Q. variabilis* under four CO_2
 636 concentrations \times five soil volumetric water contents.

^{13}C fractionation coefficients (‰)	CO_2 concentration (ppm)				
	SWC	400	500	600	800
<i>Platycladus orientalis</i>	35%–45% FC	0.0328	0.0373	0.0349	0.0332
	50%–60% FC	0.0367	0.0437	0.0382	0.0374
	60%–70% FC	0.0405	0.0366	0.0421	0.0409
	70%–80% FC	0.0444	0.0453	0.0413	0.0452
	100% FC	0.0441	0.0453	0.0456	0.0472
<i>Quercus variabilis</i>	35%–45% FC	0.0388	0.0402	0.0406	0.0384
	50%–60% FC	0.0433	0.0448	0.0409	0.0368
	60%–70% FC	0.0424	0.0440	0.0445	0.0414
	70%–80% FC	0.0424	0.0446	0.0482	0.0457
	100% FC	0.0441	0.0466	0.0466	0.0398

637

638